Tikrit Journal of Pure Science
ISSN: 1813 – 1662 (Print) --- E-ISSN: 2415 – 1726 (Online)
Journal Homepage: http://tjps.tu.edu.iq/index.php/j

Preparation and Characterization of Superparamagnetic Iron Oxide Nanoparticles (Fe_3O_4) for Biological Applications

Ahmed Hisham Fathallah [1] , Hussain S. Akbar[1] , Fatin M. Nawwab Al-Deen[2]
[1] *Physics Department , College of Education for Pure Science , University of Kirkuk , Kirkuk, Iraq*
[2] *Animal production Department , College of Agriculture. University of Kirkuk, Kirkuk, Iraq*
https://doi.org/10.25130/tjps.v26i1.103

ARTICLE INFO.
Article history:
-Received: 16 / 9 / 2020
-Accepted: 16 / 10 / 2020
-Available online: / / 2020
Keywords:
iron oxide nanoparticles, Fe_3O_4, co-precipitation method, superparamagnetic iron oxide nanoparticles SPIONs.
Corresponding Author:
Name: Ahmed Hisham Fathallah
E-mail:
ahme1993dhisham@gmail.com.
drhussainsalihakber@yahoo.com.
fatin.mn70@gmail.com
Tel:

ABSTRACT

Superparamagnetic iron oxide nanoparticles (SPIONs) are developed considering the importance of this class of in different fields of biochemical and biomedical applications owing to their distinctive chemical and physical properties. In this work, the preparation of iron oxide nanoparticles (SPIONs) using Co-precipitation method has been done as the most commonly used wet chemical method of magnetic nanoparticles preparation for biological applications. The SPIONs synthesis was based on sodium hydroxide (NaOH) mediated precipitation of Fe^{3+} and Fe^{2+} salts in an aqueous solution using trisodium citrate as surfactant within a closed system. The size and stability of the magnetite nanoparticles were carefully controlled using different chemical and physical parameters in order to obtain the SPIONs with small particle size and distribution that is needed for biomedical applications. The synthesized Fe_3O_4 nanoparticles were characterized by X-ray diffraction (XRD), scanning electron microscope (SEM), transmission electron microscope (TEM), vibrating sample magnetometer (VSM), and Zeta potential analysis (Zp). XRD pattern showed the presence of peaks corresponding to the phase of magnetite Fe_3O_4. Moreover, SEM and TEM results revealed spherical particles with a mean diameter of ≥ 5 nm. The monodispersed SPIONs were successfully prepared with a mean hydrodynamic size of 209.32 nm at a stirring speed of 900 rpm and NaOH concentration of 1.2 gm. The results showed that the particle size is considerably dependent on the stirring rate and NaOH concentration. Fe_3O_4 nanoparticles exhibited superparamagnetic behavior and the saturation magnetization was around 50 emu/g.

1. Introduction

Magnetic nanoparticles (MNPs) attracted the attention of researchers in recent years for their potential use in various applications. MNPs are solid colloidal particles ranging in size from 1 to 100 nm. MNPs have been in focus scientist at chemistry, biology, medicine, and physics [1]. Due to their dimensions comparable with those of cells, viruses, genes and proteins, they opened the potentiality of interacting with fundamental biological applications [2-5]. Iron oxide magnetic nanoparticles (SPIONs) are physically and chemically stable, biocompatible and environmentally safe, thus presenting unique characteristics for clinical applications [6].

In recent years, much attention has been paid to the synthesis of a different kinds of superparamagnetic nanoparticles (SPIONs) as nanomedical materials. Among them, engineered magnetic nanoparticles (MNPs) made of iron, cobalt, or nickel oxides exhibit special properties, including high surface-to-volume ratio and high magnetic moment, allowing potential manipulation by an external magnetic field [7].

Especially, MNPs manufactured with ferromagnetic material, i.e., superparamagnetic iron oxide nanoparticles (SPIONs), made of magnetite (Fe_3O_4) ideal biocompatibility with superparamagnetic properties allowing widespread biomedical uses such

as targeted drug delivery, bioimaging, hyperthermia, photoablation therapy, biosensors, and theranostics applications [8,9].

In general, the synthesis of SPIONs is a very critical multistep procedure, which must be optimized since its early design phase, given that even a small variation in the production process that can significantly change the desired outcome [10]. For this reason, both physical and chemical properties of the particles need to be strictly controlled in order to fit a number of different applications [11].

In recent years, researchers have focused on SPIONs preparation due to their wide applications, especially in the field of biomedical applications because of the non-toxic nature of the materials [12].

A variety of techniques have been reported to prepare SPIONs (Fe_3O_4) using different techniques such as co-precipitation [13, 14], thermal decomposition [15, 16], microemlusion, ultrasound irradiation and hydrothermal synthesis [17].

In the co-precipitation method, SPIONs (Fe_3O_4) were synthesized with the Fe^{+3} and Fe^{+2} ions in alkaline solutions, under an inert atmosphere (N_2) [18].

Some recent studies [19-23] showed the effects of many parameters for synthesis of SPIONs (Fe_3O_4).

However, in this work have attempted to prepare and synthesis SPIONs. (Fe_3O_4) using co-precipitation method and the results of investigations carried out using X-ray diffraction (XRD), scanning electron microscope (SEM), transmission electron microscope (TEM), vibrating sample magnetometer (VSM), and Zeta potential analysis (Zp).

2- Experimental part

2.1: Fabrication Techniques.

The general structure of reflux system for prepared SPIONs and the schematic was shown in Fig. 1.

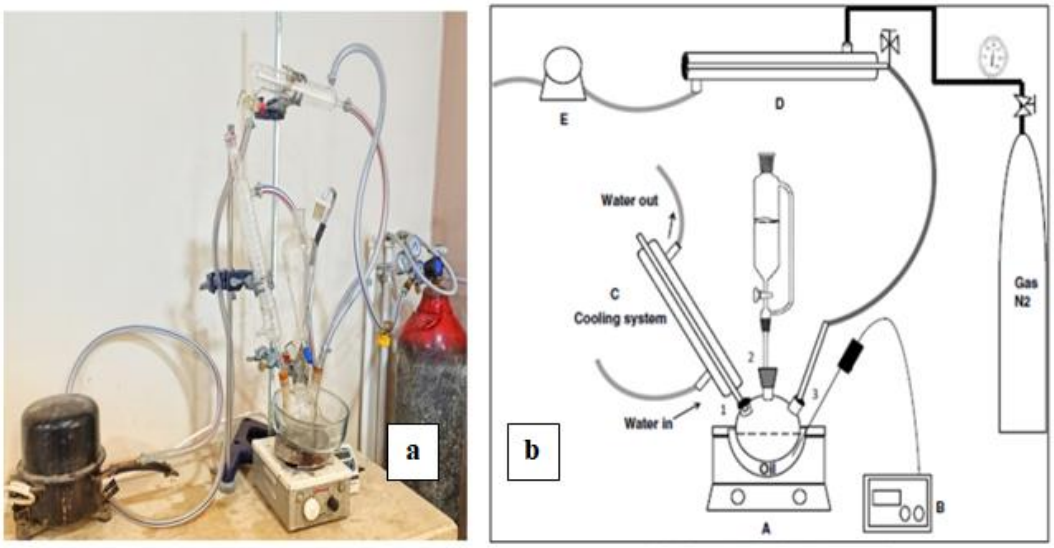

Fig. 1: (a) Photographic image of a reflux system for SPIONs. (b) Schematic structure of the reflux system for synthesis of (SPIONs). (A) Heating magnetic stirrer, (B) Digital thermometer, (C) water-cooled condenser, (E) air evacuation vacuum pump

2.2. Materials:

1.35 g of Iron (III) chloride hexahydrate ($FeCl_3.6H_2O$) and 0.69 g of Iron (II) sulfate ($FeSO_4.7H_2O$) was mixed with 1.77 g of trisodium citrate and 1.2 g of NaOH. All materials were solved with 20 milliliters deoxygenated distilled water.

2.3. Synthesis of hematite nanoparticles SPIONs.

Pure magnetite nanoparticles were synthesized with the chemical co-precipitation method .This cycle includes the joint precipitation of ferric salts and ferrous in an alkaline solution such as sodium hydroxide (NaOH) in the presence of trisodium hydroxide as a surfactant in an environment under N_2 flow as with the following chemical [24, 25]:

$$Fe^{+2} + 2Fe^{+3} + 8OH^{-1} \rightarrow Fe_3O_4 + 4H_2O \quad \ldots (1)$$

Dependence of control on the shape and size of nanoparticles is based on the ratio of Fe^{+3} and Fe^{+2}, as well as on the type of salts (for example, chloride, sulfate), and on the acidity of the medium. [26].

Fig.2 shows the flowchart for synthesis of SPIONs by co-precipitation method in the present work.

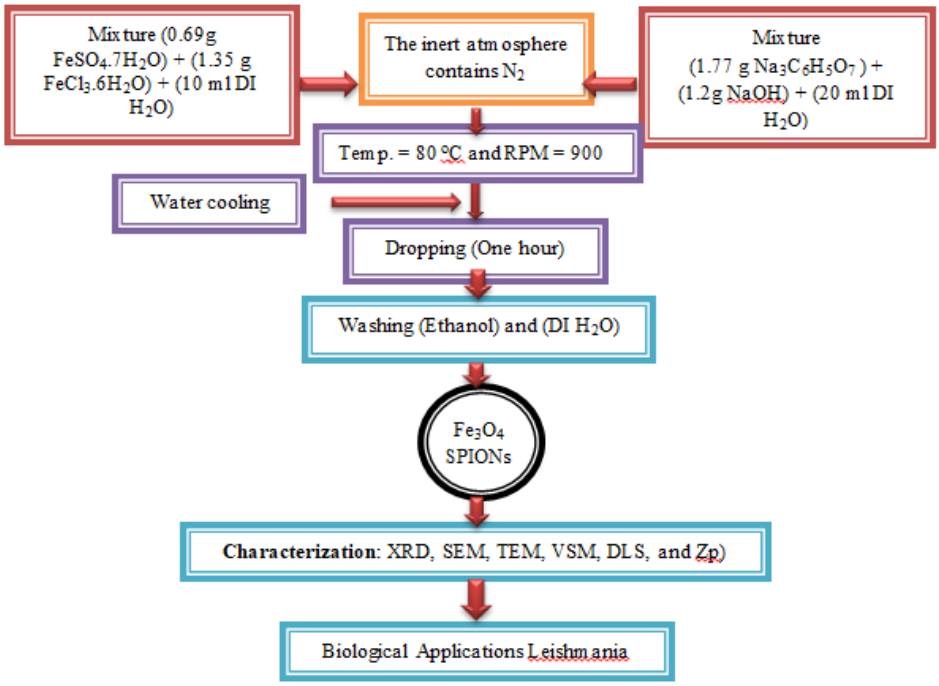

Fig. 2: Flowcharts for synthesis of SPIONs by co-precipitation method in present work.

2.4: Characterization

- **XRD characterization:**

The X-ray diffraction patterns of the samples were identified using X-ray diffractometer with CuKa radiation (1.5418 Å) as a source.

- **TEM and SEM measurements**

TEM is a versatile technique in which to analyze nanoparticle sizes, crystal structure, and morphology distribution through imaging techniques and diffraction.

The image produced by SEM was displayed on CRTs in the electronic control unit, the captured images were saved digitally or printed directly

- **Vibrating Sample Magnetometer (VSM)** the magnetic properties characterization (VSM) was used for SPIONs prepared in this work. The magnetic selection was made according to Faraday's laws so that the AC voltage is accomplished in the electrical current and equal to the rate of development of the magnetic flux through which the circuit connects, and the moment size within the sample due to the magnetic field. That the sample is swaying in a vertical direction near the detection coil if the sample fluctuation makes the AC signal at a specified frequency.

- **Zeta Potential (Zp)** measurements were used for the colloidal particles have, in most cases, a negative or positive electrostatic charge. When the electric field was shed as the particles are dispersed, the particles travel in directions and are charged in reverse. Doppler transformation occurs when particles are exposed to radiation while traveling as a result of scattering light depending on the movement of the electrophoresis. The Nano Brook program calculates the amount of Doppler shift, followed by the possibility of zeta and electrical motion, by combining a heterogeneous group and a photon subscription path to Dynamic

- **Light Scattering (DLS) (Zs)** is a device that detects the size of hydrodynamic nanoparticles. The surface of nanoparticles occurs in a variety of interactions with solvent particles and ions when the nanoparticle is surrounded by intermediates, and this strongly affects the behavior of the nanoparticles accomplish a Fourier transform (FFT) the links function obtained.

3. Esults and discussion:

3.1: X-ray diffraction analysis of SPIONs Fe_3O_4 Structure.

Fig 4. shows the X-ray diffraction (XRD) pattern of magnetite MNPs Fe_3O_4

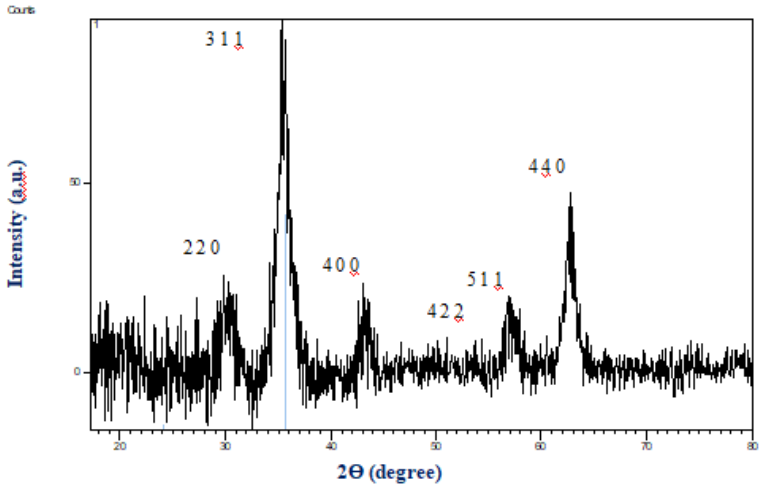

Fig. 4: X-ray diffraction for Fe_3O_4 powders spectrum prepared at 80C°, NaOH=1.2g and RPM=900.

Fig 4. shows that the character peaks of Fe_3O_4 are at $2\Theta = 29.8^o$, 35.5^o, 42.9^o, 54.38^o, 56.96^o and 62.86^o, being similar to the previously reaches for Fe_3O_4 nanoparticles [27-29]. The result of X-ray diffraction pattern indicated the magnetite (Fe_3O_4) phase. The average core size of Fe_3O_4 MNPs can be calculated to be (1.15 nm) by using Debye–Scherrer equation.

$D = K\lambda / (\beta \cos \Theta)$ …… (2)

λ is the X-ray wavelength (5.03 nm), where K is the Scherrer constant (0.92), and Θ is the Bragg diffraction angle, β is the peak full width at half maximum (FWHM) of the reflection [29].

3.2: Scanning Electron Microscope.

Fig.5 shows the scanning electron microscope (SEM) image of Fe_3O_4 MNPs prepared by the co-precipitation method at 80 °C, rotational speed 900 rpm and NaOH (1.2 g) indicating that the nanoparticles were spherical with average diameter of about (23±4) nm.

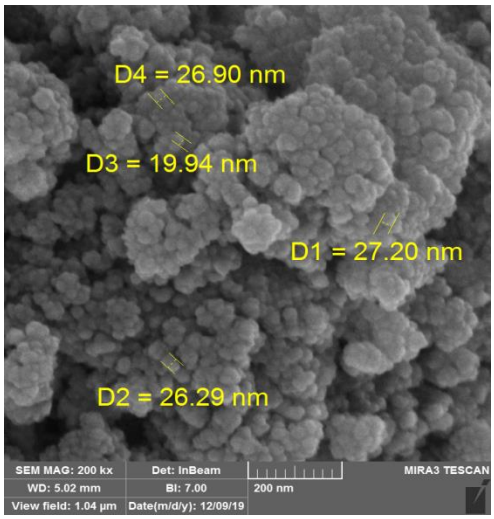

Fig. 5: SEM micrograph of Fe_3O_4 SPIONs.

When the SEM result analysis was compared with others [30]; it was found a good agreement with ref. [30].

3.3: Transmission Electron Microscopic (TEM) Analysis

Fig.6 shows the monodispersed nanoparticle which were prepared under conditions (Temp 80 °C, 900 rpm and 1.2 g NaOH) image using TEM. In order to get the actual size of MNPs (Fe_3O_4) which are prepared at 80 °C, the rotational speed 900rpm and NaOH (1.2 g) by use TEM Technique.

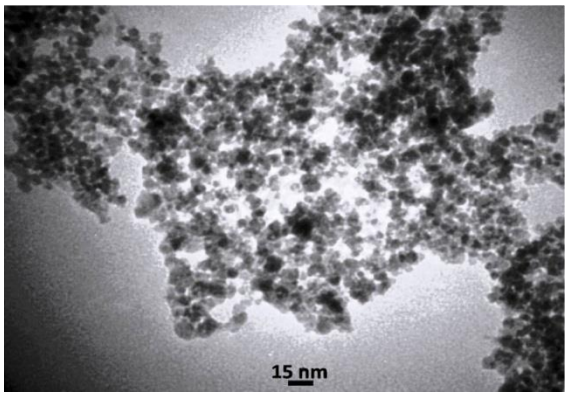

Fig. 6: Transmission electron microscopic photographs of Fe_3O_4 nanoparticles.

Fig .6 shows the magnetite Fe_3O_4 particles are spherical shape with an average diameter of (5±2) nm which is a good agreement with XRD result and also with good agreement with study indicated by [31].

3.4: Magnetic Properties Characterization (VSM) Analysis.

Vibrating sample magnetometer (VSM) was used to find the magnetic properties of Fe_3O_4 MNPs at (T=80 °C, RPM=900 and NaOH = 1.2 g) conditions.

Fig.7 shows magnetization variation of properties as a function of applied field.

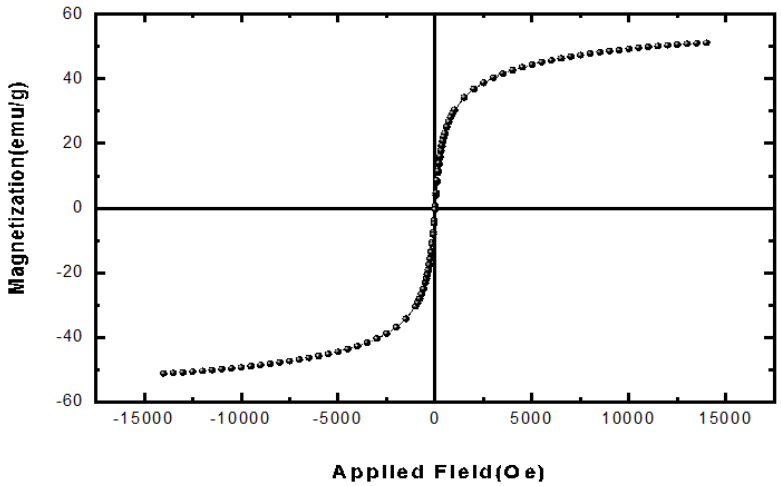

Fig. 7: The hysterias loop at 300K for Magnetization versus applied field for Fe_3O_4 obtained in present study.

Fig.7 showed the typical characteristics of superparamagnetic are observed showing almost immeasurable coercively and remanence. The saturation magnetization at which is 51.21 emu/g, is significantly less than that of the bulk magnetization [32], which is MS (bulk) 92 emu/g. The decrease in saturation is ascribed to the size effect. The magnetic particle size can also be calculated from the hysteresis curve using the following formula [33]:

$$D_m = \left(\frac{18k_BT\chi_i}{\pi\rho M_S}\right)^{1/3} \ldots\ldots (3)$$

ρ the density of Fe_3O_4(5.18 g/cm^3), where χ_i is the initial magnetic susceptibility $\chi_i = (dM/dH)_{H\to 0}$, and k_B Boltzmann constant. The initial slope near the origin was determined from the hysteresis plots by curve-fitting to the linear portion of the data. The mean magnetic particle size was calculated as (5nm), which is smaller than that observed from TEM measurement. Because a number of alternative mechanisms could result in the demagnetization of the particles, it was simplest to assume that the surface layer of magnetite atoms does not contribute to the magnetic properties of the particle [34].

Table 1 shows the comparison of SPIONs size calculated by XRD, SEM, TEM, and VSM techniques.

Table 1: Size particles comparison between XRD, SEM, TEM, and VSM techniques.

Techniques	XRD	SEM	TEM	VSM
Size(nm)	5.03	19.9	5	4.6

3.5: Zeta Size (DLS) Analysis

Dynamic light scattering (DLS) was used to determine a hydrodynamic size of SPIONs Fe_3O_4 at different rotational speeds RPM and variation concentrations of NaOH with a constant temperature of 80 ^oC. The optimum results have been observed for the Fig8, and Table 2.

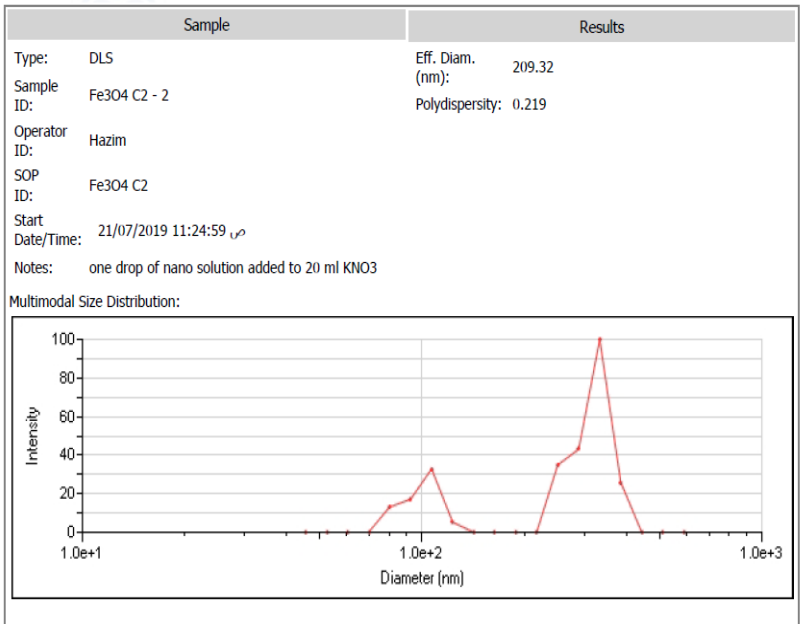

Fig. 8: Hydrodynamic size distribution of SPIONs Fe_3O_4 at RPM = 900 when NaOH= 1.2 g.

Table 2: Zeta Size variation with RPM of SPIONs Fe_3O_4.

RPM	Z_S (nm)
300	375.54
500	216.19
700	318.69
800	344.94
900	**209.32**
1300	283.76
1500	274.49

The results showed that the minimum Hydrodynamic size of Fe_3O_4 particles is 209.32 nm, when the rotational speed is 900 rpm and when the NaOH concentration is equal to1.2 gm.

Table 3 illustrate the study of changing the NaOH concentrations when the rotation speed was fixed at 900 rpm.

Table 3: Zeta Size variation of SPIONs Fe_3O_4 with NaOH concentration.

NaOH concentration	Z_S (nm)
0.72	246.59
0.96	238.51
1.2	**209.32**
1.6	1245.56

Through these results, it was found that the rotation speed RPM and sodium oxide NaOH concentrations plays an important role in determining the hydrodynamic size distribution DLS of nanoparticles SPIONs and that the optimum value in the rotation speed was 900 rpm and the 1.2g of NaOH concentration. The hydrodynamic volumes obtained are greater than those observed by TEM, this due to the absence of an external magnetic field, static magnetic interactions (dipole magnetic dipole) between the particles can cause their agglomeration [35].

3.5: Zeta Potential Analysis

Zp variation with speed rotation of solution (RPM).

Colloidal stability (Zp) of the nanoparticles SPIONs plays very significant role in introducing them to *in vivo* biological applications. Table 4 shows the results of variations of Zp with a different speed of rotation of solutions RPM at certain of concentrations NaOH(1.2g).

Table 4. Zeta Potential variation with RPM of SPIONs Fe_3O_4.

RPM	Z_P (mV)
300	-27.99
500	-17.24
700	-27.55
800	-23.29
900	**-22.37**
1300	-30.35
1500	-18.19

Fig. 9 shows the variations of Zp when the speed of rotation of solutions RPM at 900 and at a certain of concentrations NaOH(1.2g).

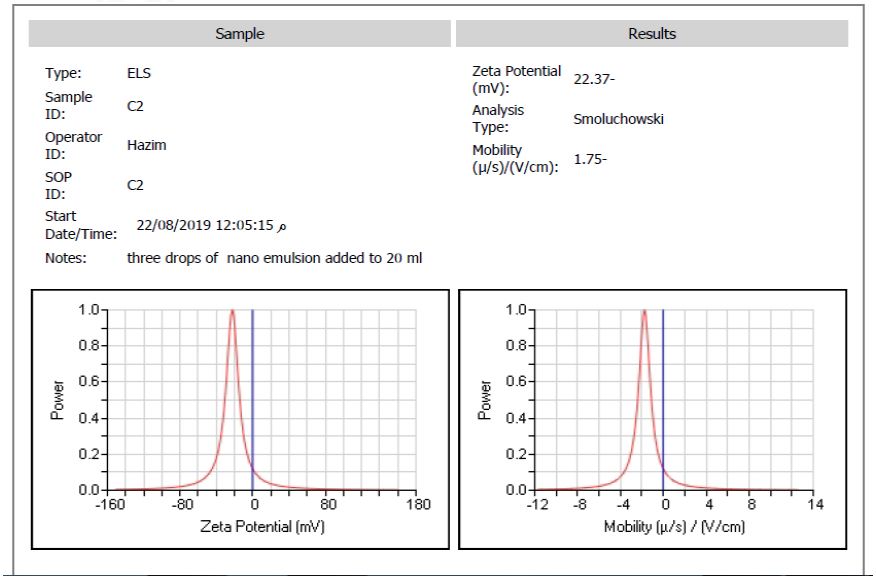

Fig. 9: Zeta Potential variation of SPIONs Fe_3O_4 at 900 RPM and NaOH=1.2g.

Fig .9 shows from the results that the Zeta Potential variation of Fe_3O_4 is about (-22 mv) at 900 RPM.

Zp variation with NaOH concentrations.

Table 5 shows the results of variations of Zp at concentrations NaOH when the speed of rotation of solutions at 900 rpm.

Table 5: Zeta Potential variations of SPIONs Fe_3O_4 at different NaOH.

NaOH (g)	Z_P (mV)
0.72	-27.28
0.96	-26.44
1.2	**-22.37**
1.6	-24.53

Fig.10 shows the variations of Zp at a constant speed of rotation with 1.2 g of NaOH.

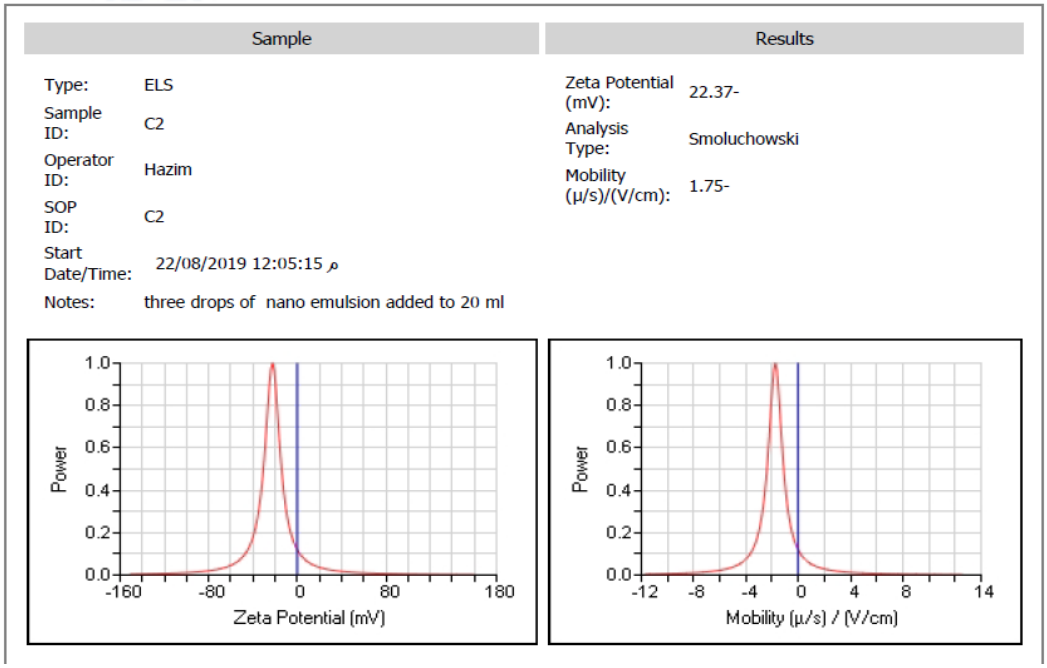

Fig. 10: Zeta Potential variation of SPIONs Fe_3O_4 at 1.2 g of NaOH and RPM=900.

The results observed that Fe_3O_4 SPOINs nanoparticles have negative zeta potential -22.37 mV. Thus, it can be concluded that the nanoparticles are sufficiently stable. Hence, the more negative and stable materials are highly more suitable for biological applications [36].

4. Conclusions

The main conclusions that may be drawn from this work are:

1- The Co-precipitation method allows producing large number of hydrolytic nanoparticles Fe_3O_4 SPIONs per batch.

2- The results showed that the crystalline and average particle size of SPIONs (Fe_3O_4) depends on stirring speed and the concentration of NaOH.

3- The saturation magnetization of SPIONs Fe_3O_4 was proportional to the particle size.

4- The synthesized SPIONs have an average diameter (5) nm as evidenced by TEM technique when the co-precipitation technique controlled to produce SPIONs Fe_3O_4 using (1.2g NaOH), and are revealed to be ideal for *in viro* and *in vivo* studies.

5- XRD showed the crystalline phase corresponds to magnetite (Fe_3O_4). The spectra showed that the SPIONs are in super magnetic state.

6- The magnetization measurements as a function of the magnetic field showed a typical behavior of superparamagnetic iron oxide nanoparticles SPIONs in material because there was no correctively in the hysteric's loop.

7- The nanoparticles SPIONs synthesized during this work are ready and has potential for biocompatibility studies.

References

[1] McNamara, K., & Tofail, S. A. (2015). Nanosystems: the use of nanoalloys, metallic, bimetallic, and magnetic nanoparticles in biomedical applications. *Physical chemistry chemical physics*, **17(42):** 27981-27995.

[2] Riviere, C., Roux, S., Tillement, O., Billotey, C., & Perriat, P. (2006). Nano-systems for medical applications: biological detection, drug delivery, diagnosis and therapy. *Annales de Chimie. Science des Materiaux (Paris)*, **31(3):** 351-367.

[3] Suri, S. S., Fenniri, H., & Singh, B. (2007). Nanotechnology-based drug delivery systems. *Journal of occupational medicine and toxicology*, **2(1):** 16-21.

[4] Ochekpe, N. A., Olorunfemi, P. O., & Ngwuluka, N. C. (2009). Nanotechnology and drug delivery part 1: background and applications. *Tropical journal of pharmaceutical research*, **8(3):** 265-274.

[5] Niemirowicz, K., Markiewicz, K.H., Wilczewska, A. Z., & Car, H. (2012). Magnetic nanoparticles as new diagnostic tools in medicine. *Advances in medical sciences*, **57(2)**: 196-207.

[6] Wilczewska, A. Z., Niemirowicz, K., Markiewicz, K. H., & Car, H. (2012). Nanoparticles as drug delivery systems. *Pharmacological reports*, **64(5):** 1020-1037.

[7] Lu, A. H., Salabas, E. E., & Schüth, F. (2007). Magnetic nanoparticles: synthesis, protection, functionalization, and application. *Angewandte Chemie International Edition*, **46(8):** 1222-1244.

[8] Cardoso, V. F., Francesko, A., Ribeiro, C., Bañobre- López, M., Martins, P., & Lanceros-Mendez, S. (2018). Advances in magnetic nanoparticles for biomedical applications. *Advanced healthcare materials*, **7(5):** 1700845-1700879.

[9] Khanna, L., Verma, N. K., & Tripathi, S. K. (2018). Burgeoning tool of biomedical applications-Superparamagnetic nanoparticles. *Journal of Alloys and Compounds*, **752:** 332-353.
[10] Xie, W., Guo, Z., Gao, F., Gao, Q., Wang, D., Liaw, B. S., ... & Zhao, L. (2018). Shape-, size-and structure-controlled synthesis and biocompatibility of iron oxide nanoparticles for magnetic theranostics. *Theranostics*, **8(12):** 3284-3307.
[11] Majidi, S., Zeinali Sehrig, F., Farkhani, S. M., Soleymani Goloujeh, M., & Akbarzadeh, A. (2016). Current methods for synthesis of magnetic nanoparticles. *Artificial cells, nanomedicine, and biotechnology*, **44(2):** 722-734.
[12] Bhandari, R., Gupta, P., Dziubla, T., & Hilt, J. Z. (2016). Single step synthesis, characterization and applications of curcumin functionalized iron oxide magnetic nanoparticles. *Materials Science and Engineering:* **C, 67:** 59-64.
[13] Jolivet, J. P., Chanéac, C., & Tronc, E. (2004). Iron oxide chemistry. From molecular clusters to extended solid networks. *Chemical communications*, **(5):** 481-483.
[14] Mascolo, M. C., Pei, Y., & Ring, T. A. (2013). Room temperature co-precipitation synthesis of magnetite nanoparticles in a large pH window with different bases. *Materials*, **6(12):** 5549-5567.
[15] Park, J., An, K., Hwang, Y., Park, J. G., Noh, H. J., Kim, J. Y., ... & Hyeon, T. (2004). Ultra-large-scale syntheses of monodisperse nanocrystals. *Nature materials*, **3(12):** 891-895.
[16] Bee, A., Massart, R., & Neveu, S. (1995). Synthesis of very fine maghemite particles. *Journal of Magnetism and Magnetic Materials*, **149(1-2):** 6-9.
[17] Teo, B. M., Chen, F., Hatton, T. A., Grieser, F., & Ashokkumar, M. (2009). Novel one-pot synthesis of magnetite latex nanoparticles by ultrasound irradiation. *Langmuir*, **25(5):** 2593-2595.
[18] Yan, H., Zhang, J., You, C., Song, Z., Yu, B., & Shen, Y. (2009). Influences of different synthesis conditions on properties of Fe3O4 nanoparticles. *Materials Chemistry and Physics*, **113(1):** 46-52.
[19] Gupta, A. K., & Gupta, M. (2005). Synthesis and surface engineering of iron oxide nanoparticles for biomedical applications. *biomaterials*, **26(18):** 3995-4021.
[20] Valenzuela, R., Fuentes, M. C., Parra, C., Baeza, J., Duran, N., Sharma, S. K., ... & Freer, J. (2009). Influence of stirring velocity on the synthesis of magnetite nanoparticles (Fe3O4) by the co-precipitation method. *Journal of Alloys and Compounds*, **488(1):** 227-231.
[21] Kandpal, N. D., Sah, N., Loshali, R., Joshi, R., & Prasad, J. (2014). Co-precipitation method of synthesis and characterization of iron oxide nanoparticles. *Journal of Scientific and Industrial Research* ,**73:**87-90
[22] Malhotra, A., Spieß, F., Stegelmeier, C., Debbeler, C., & Lüdtke-Buzug, K. (2016). Effect of key parameters on synthesis of superparamagnetic nanoparticles (SPIONs). *Current Directions in Biomedical Engineering*, **2(1):** 529-532.
[23] Daoush, W. M. (2017). Co-precipitation and magnetic properties of magnetite nanoparticles for potential biomedical applications. *J. Nanomed. Res*, **5(3):** 00118.
[24] Massart, R. (1981). Preparation of aqueous magnetic liquids in alkaline and acidic media. *IEEE transactions on magnetics*, **17(2):** 1247-1248.
[25] Massart, R., Dubois, E., Cabuil, V., & Hasmonay, E. (1995). Preparation and properties of monodisperse magnetic fluids. *Journal of Magnetism and Magnetic Materials*, **149(1-2):** 1-5.
[26] Gupta, A. K., & Gupta, M. (2005). Synthesis and surface engineering of iron oxide nanoparticles for biomedical applications. *biomaterials*, **26(18):** 3995-4021.
[27] Iida, H., Takayanagi, K., Nakanishi, T., & Osaka, T. (2007). Synthesis of Fe3O4 nanoparticles with various sizes and magnetic properties by controlled hydrolysis. *Journal of colloid and interface science*, **314(1):** 274-280.
[28] Mizukoshi, Y., Shuto, T., Masahashi, N., & Tanabe, S. (2009). Preparation of superparamagnetic magnetite nanoparticles by reverse precipitation method: contribution of sonochemically generated oxidants. *Ultrasonics sonochemistry*, **16(4):** 525-531.
[29] Yan, H., Zhang, J., You, C., Song, Z., Yu, B., & Shen, Y. (2009). Influences of different synthesis conditions on properties of Fe3O4 nanoparticles. *Materials Chemistry and Physics*, **113(1):** 46-52.
[30] Arsalani, N., Fattahi, H., & Nazarpoor, M. (2010). Synthesis and characterization of PVP-functionalized superparamagnetic Fe3O4 nanoparticles as an MRI contrast agent. *Express Polym Lett*, **4(6):** 329-38.
[31] Liang, Y. Y., & Zhang, L. M. (2007). Bioconjugation of papain on superparamagnetic nanoparticles decorated with carboxymethylated chitosan. *Biomacromolecules*, **8(5):** 1480-1486.
[32] Han, D. H., Wang, J. P., & Luo, H. L. (1994). Crystallite size effect on saturation magnetization of fine ferrimagnetic particles. *Journal of Magnetism and Magnetic Materials*, **136(1-2):** 176-182.
[33] Massart, R. (1981). Preparation of aqueous magnetic liquids in alkaline and acidic media. *IEEE transactions on magnetics*, **17(2):** 1247-1248.
[34] Liu, Z. L., Liu, Y. J., Yao, K. L., Ding, Z. H., Tao, J., & Wang, X. (2002). Synthesis and magnetic properties of Fe 3 O 4 nanoparticles. *Journal of materials synthesis and processing*, **10(2):** 83-87.
[35] Mahmoudi, M., Simchi, A., Milani, A. S., & Stroeve, P. (2009). Cell toxicity of superparamagnetic iron oxide nanoparticles. *Journal of colloid and interface science*, **336(2):** 510-518.
[36] Delener. M. (2013). Prepearing solutions of containing iron oxide nanoparticles to improve heat transfer**.** *Msc Thesis, Marmara University Institute for Graduate Studies in Pure and Applied.*

تحضير وتشخيص الجسيمات النانوية لأوكسيد الحديد المغناطيسي (مغنيتايت Fe_3O_4) للتطبيقات البايولوجية

احمد هشام فتح الله[1] ، حسين صالح أكبر[1] ، فاتن محمد نواب الدين[2]

[1] قسم الفيزياء ، كلية التربية للعلوم الصرفة ، جامعة كركوك ، كركوك ، العراق

[2]قسم الانتاج الحيواني ، كلية الزراعة ، جامعة كركوك ، كركوك ، العراق

الملخص

تم تطوير الجسيمات النانوية الفائقة المغناطيسية (SPIONs) مع الأخذ في الاعتبار أهمية هذه الفئة من المواد الوظيفية غير المادية في مجالات مختلفة من التطبيقات الكيميائية الحيوية والطبية الحيوية نظرًا لخصائصها الكيميائية والفيزيائية المميزة. في هذه الدراسة، تم تحضير جسيمات أكسيد الحديد النانوية SPIONs (باستخدام طريقة الترسيب المشترك) باعتبارها الطريقة الكيميائية الرطبة الأكثر استخدامًا لإعداد الجسيمات النانوية المغناطيسية للتطبيقات البيولوجية. تطلبت هذه التطبيقات أن SPIONs مثل أكسيد الحديد Fe_3O_4 الجسيمات النانوية المغناطيسية (أكسيد الحديد الأسود) الذي يحتوي على قيم مغنطة عالية وحجم جزيئات أصغر من 100 نانومتر.

في هذه الدراسة تم تحضير وبناء SPIONs بترسيب هيدروكسيد الصوديوم (NaOH) بوساطة أملاح Fe^{+3} وFe^{+2} في محلول مائي باستخدام حامض سترات الصوديوم كمواد خافض للتوتر السطحي داخل نظام مغلق بوجود غاز النيتروجين N_2. في الدراسة تم التحكم بدقة في حجم واستقرار الجسيمات النانوية المغناطيسية باستخدام معايير كيميائية وفيزيائية مختلفة من أجل الحصول على SPIONs ذات حجم وتوزيع جزيئات صغير مهمة للتطبيقات الطبية الحيوية.

تم هنا وصف التفاصيل التجريبية للحصول على Fe_3O_4 غير مصقول أحادي التشتت عند درجة حرارة 80 درجة مئوية مع سرعات دوران مختلفة وتركيزات هيدروكسيد الصوديوم. تميزت الجسيمات النانوية التي تم الحصول عليها من خلال الفحص المجهري الإلكتروني (TEM)، والمسح المجهري الإلكتروني (SEM)، وحيود مسحوق الأشعة السينية (XRD)، ومقياس المغناطيسية لعينة الاهتزاز (VSM)، وتحليل جهد زيتا (Zp).

أظهرت النتائج أن حجم الجسيمات يعتمد بشكل كبير على معدل التحريك وتركيز هيدروكسيد الصوديوم. تم تحضير SPIONs أحادية التشتت بنجاح بمتوسط حجم هيدروديناميكي قدره 209.32 نانومتر عند سرعة التحريك 900 دورة في الدقيقة وتركيز هيدروكسيد الصوديوم 1.2 غم. أظهرت جزيئات Fe_3O_4 النانوية المُصنَّعة سلوكًا مغناطيسيًا فائقًا وكان مغنطة التشبع حوالي 50 emu/g. كشف فحص الجسيمات بواسطة TEM و SEM عن جسيمات كروية يبلغ متوسط قطرها ≤ 5 نانومتر. بينما أظهر نمط XRD وجود قمم مطابقة لمرحلة أكسيد الحديد الأسود.